ChemPubSoc Europe

DOI: 10.1002/cbic.201900559

CHEMBIOCHEM Communications

A Genetically Encoded Diazirine Analogue for RNA–Protein Photo-crosslinking

Dmytro Dziuba,*[a] Jan-Erik Hoffmann,[a, b] Matthias W. Hentze,[a] and Carsten Schultz*[a, b]

Ultraviolent crosslinking is a key experimental step in the numerous protocols that have been developed for capturing and dissecting RNA–protein interactions in living cells. UV crosslinking covalently stalls dynamic interactions between RNAs and the directly contacting RNA-binding proteins and enables stringent denaturing downstream purification conditions needed for the enrichment and biochemical analysis of RNA–protein complexes. Despite its popularity, conventional 254 nm UV crosslinking possesses a set of intrinsic drawbacks, with the low photochemical efficiency being the central caveat. Here we show that genetically encoded photoreactive unnatural amino acids bearing a dialkyl diazirine photoreactive group can address this problem. Using the human iron regulatory protein 1 (IRP1) as a model RNA-binding protein, we show that the photoreactive amino acids can be introduced into the protein without diminishing its RNA-binding properties. A sevenfold increase in the crosslinking efficiency compared to conventional 254 nm UV crosslinking was achieved using the diazirine-based unnatural amino acid DiAzKs. This finding opens an avenue for new applications of the unnatural amino acids in studying RNA–protein interactions.

RNA-binding proteins (RBPs) are ubiquitous cellular factors associated with virtually all cellular RNAs through every stage of their lifecycle. RBPs can alter splicing, processing, localization, stability, translation and functioning of the bound RNAs, and therefore are involved in the regulation of gene expression at multiple levels.[1] Reliable mapping of RBP-RNA interactions from both a RNA-centric and a protein-centric perspective has been a long-standing challenge in RNA biology.[2] A set of analytical biochemical techniques has been developed to address this problem.[3] Among them, the RNA interactome capture (RIC) technique has served to reveal interactions between polyadenylated RNAs and proteins at the whole-proteome level,[4] whereas a family of crosslinking immunoprecipitation (CLIP) methods has been developed to identify RNA targets of a selected RBP of interest.[5] The key experimental step shared by both techniques is ultraviolet crosslinking (UV crosslinking) of RBPs to the RNAs they directly interact with. The excitation of the RNA nucleobases with 254 nm UV light generates reactive intermediates and stochastically creates new covalent bonds with amino acid residues of the bound RBPs.[6] Therefore, UV crosslinking stalls interaction dynamics and covalently links the interacting partners together in a way that withstands stringent denaturing downstream enrichment and analysis steps. The introduction of UV crosslinking has revolutionized the field and boosted high-throughput studies of RPBs and RNA-protein interactions.[3b,7] At the same time, conventional UV crosslinking possesses a range of intrinsic drawbacks which limit the performance of the experimental procedures.[7] For instance, the chemical yield of the photo-crosslinking step is typically very low (<1%). Also, 254 nm UV light produces undesirable intra- and interstrand RNA-RNA crosslinks and phosphodiester backbone breaks.[8] Moreover, 254 nm UV crosslinking has an inherent bias coming from the unequal photochemical reactivity of different nucleobases toward different amino acid side chains and also from different reactivity of structured and unstructured stretches of RNA.[6,7] The mentioned factors complicate both the processing of crosslinked samples and interpretation of the results. A number of techniques have been introduced to address these drawbacks by increasing the photoreactivity of RNAs. For instance, photoactivatable ribonucleoside-enhanced crosslinking (PAR-CL) is based on the labeling of cellular RNAs with photoreactive thionucleosides such as 4-thiouridine (4SU).[9] In addition to that, a range of synthetic nucleoside analogues bearing artificial photoreactive crosslinkers has been proposed for the enhanced crosslinking of RNAs with their interactors.[10] At the same time, new ways to improve the photoreactivity of RBPs themselves are still needed.

Genetic code expansion techniques,[11] such as the amber stop codon suppression, have enabled programmable site-selective co-translational labeling of proteins with a wide range of unnatural amino acids (uAAs) bearing chemically diverse side chains.[12] Unnatural amino acids featuring photoreactive side chains have gained popularity as tools for efficient covalent capturing of biomolecular interactions in the fields of chemical proteomics and interactomics.[13] It is worth noting, that in the vast majority of the reports, the focus had been set on applying genetically encoded photoactive unnatural amino acids for capturing protein-peptide and protein-protein inter-

[a] Dr. D. Dziuba, Dr. J.-E. Hoffmann, Prof. M. W. Hentze, Prof. C. Schultz
European Molecular Biology Laboratory
Meyerhofstrasse 1, 69117 Heidelberg (Germany)
E-mail: dziuba@embl.de

[b] Dr. J.-E. Hoffmann, Prof. C. Schultz
Department of Chemical Physiology and Biochemistry
Oregon Health and Science University
L334, 3181 SW Sam Jackson Park Road, Portland, OR 97239-3098 (USA)
E-mail: schulcar@ohsu.edu

Supporting information and the ORCID identification numbers for the authors of this article can be found under https://doi.org/10.1002/cbic.201900559.

This article is part of a Special Issue commemorating the 20th Anniversary of ChemBioChem. To view the complete issue, visit our homepage

actions.[14] Here we show that genetically encodable photoreactive unnatural amino acids can be used for enhanced site-selective RNA-protein photo-crosslinking. This approach is provisioned to be beneficial over conventional 254 nm UV crosslinking for the following reasons: 1) Excitation with longer wavelengths will decrease undesirable side-reactions and 2) designed photo-crosslinking groups are expected to generate larger amounts of photo-crosslinking products relative to UV-activated natural nucleobases. We chose two diazirine-based pyrrolysine analogues and focused on the iron regulatory protein 1 (IRP1) as a model RNA-binding protein. We studied the effect of the unnatural amino acid mutagenesis on its RNA-binding properties and then performed side-by-side comparison of the efficiency of diazirine-mediated crosslinking relative to conventional 254 nm UV crosslinking.

Over a dozen photoreactive unnatural amino acids have been described in the literature, bearing a relatively small number of photo-crosslinking chemical moieties.[12b,13] Those include aliphatic and aromatic diazirines, benzophenones and several other photochemically active scaffolds. For this study, we decided to focus on alkyl diazirine-based crosslinkers because of their small molecular size, the favorable photoactivation kinetics and the versatility of the carbene-mediated crosslinking chemistry.[15] We selected two diazirine-based analogues of pyrrolysine (Figure 1 A) based on our own previous work and on literature reports.[16,17] The unnatural amino acid DiAzKs is a pyrrolysine analogue bearing an alkyl diazirine reactive group attached via a short flexible C2 linker. This unnatural amino acid has been shown to be proficient in protein-protein crosslinking.[16] The second selected unnatural amino acid called PrDiAzK is a pyrrolysine analogue featuring a combination of the same photoreactive diazirine group with a reactive propargyl handle which is amenable to derivatization using the Cu-catalyzed azide–alkyne cycloaddition. This amino acid has been shown to crosslink interacting proteins, whereas the reactive handle might be useful for the derivatization of labeled proteins and crosslinked complexes with a fluorophore or for affinity tagging followed by purification and analysis of the conjugates.[17] We previously demonstrated that both amino acids are readily genetically encodable using the double AF mutant of pyrrolysine aminoacyl-tRNA synthetase from archaea *Methanosarcina mazei* (*Mm*PylRS^{AF}).[17] A state-of-the-art genetic code expansion system based on the expression of the Y39 amber mutant of green fluorescent protein (GFP) as a reporter in bacteria *Escherichia coli* BL21-AI[18] was used for these experiments. The full-length GFP was isolated only when an additional unnatural amino acid was added to the growth medium (Figure 1 B, lanes 2–4). Notably, the yield of the recombinant GFP was higher in the case of the selected diazirine-based unnatural amino acids than with N_ε-Boc-L-lysine (BocK, Figure S1 in the Supporting Information), a widely used reference unnatural amino acid. Next, we confirmed that the propargyl group of the unnatural amino acid PrDiAzK can be derivatized using Cu^I-catalyzed click chemistry (Figure 1 C). When purified recombinant uAA mutants of GFP were incubated with fluorescent 5-carboxytetramethylrhodamine-PEG_3-azide (TAMRA-N_3, Figure S1) in the presence or in the absence of Cu^I catalyst, the formation of fluorophore-protein conjugate was observed only for the PrDiAzK mutant and only in the presence of the catalyst (Figure 1 C, lane 6).

Next, we studied the impact of unnatural amino acid incorporation on the RNA-binding properties of a canonical RNA-binding protein. We focused on the human iron regulatory protein 1 (IRP1), also known as cytosolic aconitase (ACO1), a key factor involved in the regulation of intracellular iron homeostasis.[19] IRP1 is a 100 kDa multidomain cytosolic protein which binds to an RNA motif called the iron responsive element (IRE), a conserved ≈30-nucleotide stem–loop structure found in the untranslated regions (UTRs) of transcripts of genes encoding key proteins in iron metabolism. We inspected the available crystal structure of an IRP1–IRE complex [20] (PDB ID: 3SNP) and selected two amino acid residues in close proximity to the bound RNA molecule, potentially suitable for the incorporation of the diazirine crosslinker amino acids. These

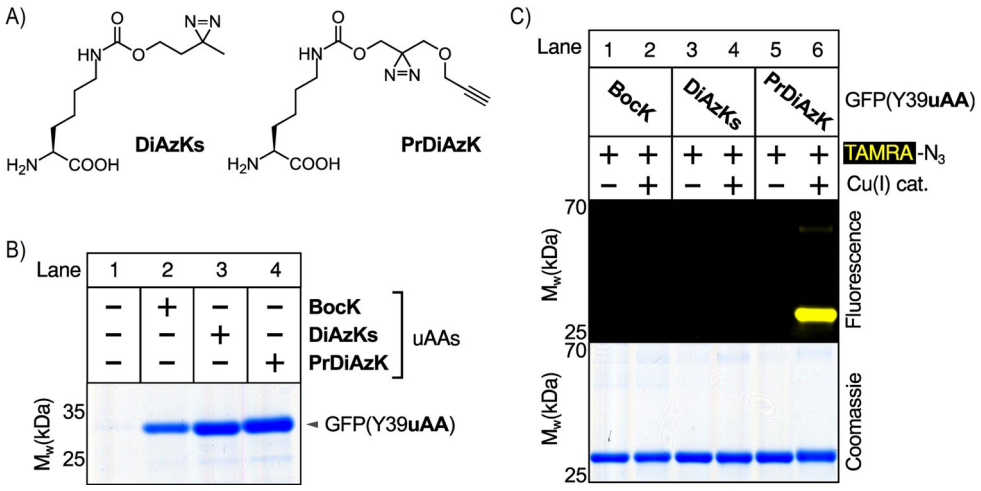

Figure 1. A) Chemical structures of the diazirine-based photo-crosslinkable unnatural amino acids used in this study. B) Bacterial expression and affinity purification of the Y39 amber mutant of green fluorescent protein upon amber codon suppression; SDS-PAGE, Coomassie staining. C) The click-labeling of the uAA-labeled recombinant GFP using the Cu^I-catalyzed azide–alkyne cycloaddition; SDS-PAGE, in-gel fluorescence (λ_{ex} = 532 nm) and Coomassie staining.

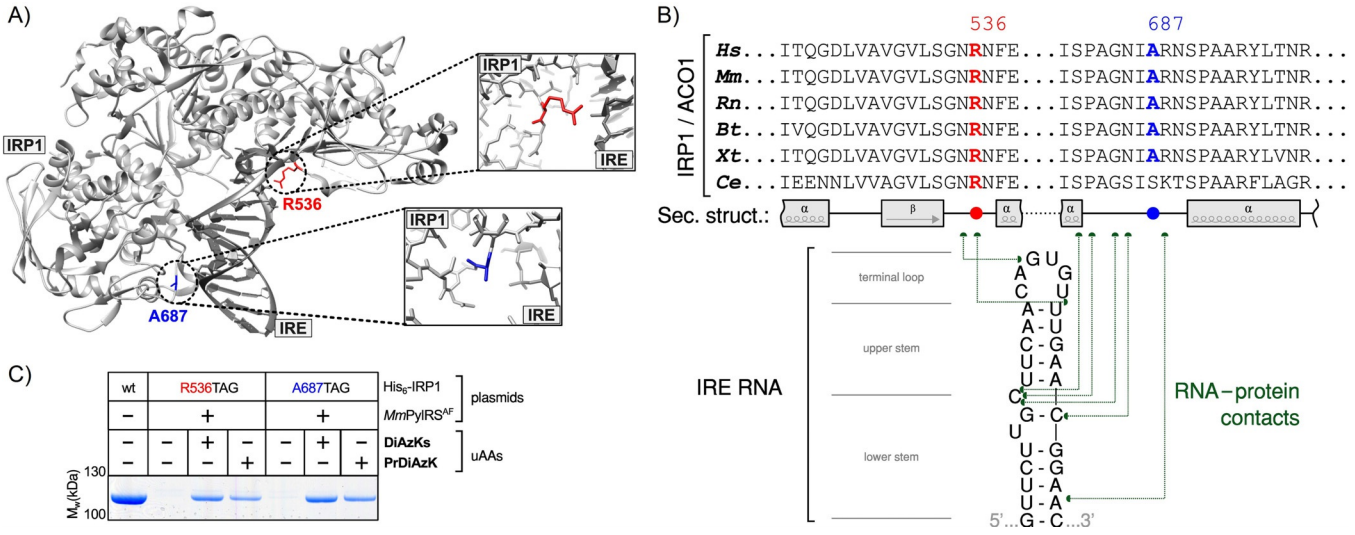

Figure 2. A) The structure of iron-regulating protein 1 (IRP1) bound to an iron-responsive element (IRE) of ferritin H; PDB ID: 3SNP. Amino acid positions R536 and A687 selected for the insertion of the diazirine photo-crosslinkers are highlighted in red and blue, respectively; the insets show the contacts of R536 and A687 to the RNA backbone. B) Partial sequence alignment of the human (*Homo sapiens*, *Hs*) IRP1 with its homologues in other species. *Ms* = *Mus musculus*, *Rn* = *Rattus norvegicus*, *Bt* = *Bos taurus*, *Xt* = *Xenopus tropicalis*, *Ce* = *Caenorhabditis elegans*. The rectangles and the line below the sequences correspond to the structured and unstructured elements in the human IRP1 according to PDB ID: 3SNP; the protein–RNA contacts present in that structure are mapped by dotted lines. C) Bacterial expression and affinity purification of the wild-type and uAA mutants of the human IRP1.

amino acids were Arg536 and Ala687 making nonspecific contacts to the sugar-phosphate backbone (Figure 2A). We performed additional analysis to assess the suitability of the selected positions for the incorporation of the photo-crosslinkers. In a recent study, Kohli and co-workers reported [21] that factors such as conservation, hydrophobicity, or accessibility cannot be used as predictors of the tolerability of proteins toward the unnatural amino acid mutagenesis. At the same time, the overall position of the incorporated unnatural amino acid within the secondary and tertiary protein fold was shown to be highly relevant. Despite the fact that positions which we selected are conserved in vertebrates (A687) or in vertebrates and invertebrates (R536), they lie outside of the local folded secondary structure elements and are located within unfolded loops (Figure 2B). We speculated that they therefore are less likely to destabilize overall protein folding and stability. Because both flexible loops form several protein–RNA contacts with the IRE RNA (Figure 2B), multiple crosslinking-favorable molecular contacts of the photoactivated diazirine amino acids with the RNA can be anticipated for both the R536 and A687 mutants.

To test RNA-binding properties of the selected uAA mutants of IRP1, we first expressed human recombinant wild-type IRP1 in bacteria and purified it using an N-terminal polyhistidine affinity tag according to the literature procedure[22] with several modifications. We found that the bacterial strain *E. coli* NiCo21(DE3) engineered for the facile purification of polyhistidine-tagged proteins[23] is a convenient host for the production and purification of the recombinant IRP1. The amber mutant plasmids having an in-frame amber stop codon (TAG) at amino acid positions 536 and 687 were also generated by site-directed mutagenesis for the expression of the unnatural amino acid mutants of IRP1. Full-length IRP1 was expressed in bacteria carrying an amber mutant IRP1 plasmid and the amber suppression plasmid with the *Mm*PylRS^{AF} synthetase only when one of the diazirine unnatural amino acids was added to the growth media (Figure 2C), thereby giving access to recombinant IRP1 bearing a site-selectively incorporated photo-crosslinker.

Next, we investigated whether the unnatural amino acid-bearing mutants of IRP1 bind to RNA. We performed an electrophoretic mobility shift assay (EMSA). Increasing amounts of recombinant IRP1 were added to a radioactively labeled RNA probe corresponding to the IRE from the 5′-UTR of the human ferritin heavy chain mRNA (FTH-IRE). The IRP1–IRE complex was separated from the free probe by native gel electrophoresis. We found that the unnatural amino acid mutants of IRP1 interact with the FTH-IRE similarly to the wild-type IRP1 as shown in Figure 3A for the A687DiAzKs mutant. For quantification, we measured K_d values of IRP1–IRE binding for the wild-type protein and for the four unnatural amino acid mutants. An IRP1 mutant reported to have significantly decreased RNA binding (R780Q) was used as a negative control.[24] Using the EMSA assay, a K_d value of 18 ± 5 nM for the wild-type IRP1 expressed in bacteria was obtained, which is close to the value reported previously for the recombinant IRP1 expressed in yeast (12–14 nM).[25] The negative control R780Q mutant bound to the same RNA probe weaker (Figure S2), with the observed K_d value being about 20-fold higher than the wild-type protein, in line with literature data.[24] More importantly, we observed no increase in K_d for the four studied unnatural amino acid mutants of IPR1. Particularly, the K_d value obtained for the R536DiAzKs mutant was about fourfold lower than the wild-type protein, whereas the K_d values obtained for R536PrDiAzK and both A687 mutants were nearly the same as for the wild-type protein. Altogether, these results indicate that the select-

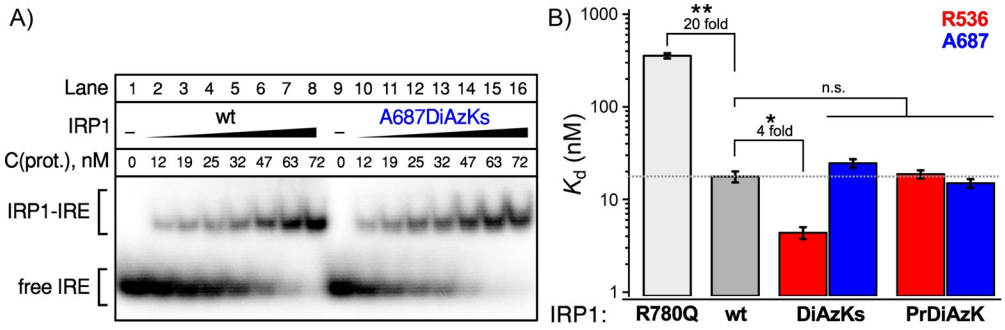

Figure 3. A) Electrophoretic mobility shift assay (EMSA) shows that both the wild-type and uAA-labeled IRP1 bind to the ferritin heavy chain IRE (FTH-IRE) RNA; native PAGE, radioautography. B) K_d values obtained from the EMSA assay for the wild-type IRP1, the R780Q mutant (a negative control having decreased RNA binding) and for the studied unnatural amino acid mutants of IRP1; $^*p<0.05$, $^{**}p<0.01$, n.s.: not significant.

ed diazirine-based amino acids can be incorporated into an RNA-binding protein without affecting its ability to bind RNA.

Binding specificity, or in other words the ability of RNA-binding proteins to discriminate between alternative binding sites in RNAs, is an important aspect of RNA-protein recognition.[26] The IRP1 is known to bind to a range of IRE variants differing in the stem region, whereas a single nucleotide deletion within the highly conserved terminal loop region has been shown to destabilize binding and to induce a loss of function.[27] We examined whether the insertion of the diazirine-based amino acid affects the ability of the IRP1 to discriminate between correct and defective IRE RNA variants. A defective FTH-IRE RNA probe lacking the key cytidine residue[27] required for the IRP1 binding (Figure 4A and Table S1) was used and referred to as IRE-ΔC. The mobility shift assay was performed at equal concentrations of IRE-wt and IRE-ΔC and equal concentrations of five IRP1 proteins (wild-type with the four uAA mutants). As shown in Figure 4B, the wild-type IRP1 binds to the IRE-ΔC probe weaker than to the wild-type IRE, resulting in a ≈five-fold increase of the fraction of unbound RNA (lane 8 compared with lane 2). At the same time, the differential binding to the IREs was affected for the four diazirine-bearing mutants to different extents (lanes 9–12 compared with lanes 3–6). Quantification (Figure 4C) showed that only the R536DiAzKs mutant exhibited significantly lower binding specificity than the wild-type protein, whereas for the other three protein the decrease in binding specificity was insignificant. Altogether, this experiment demonstrates that the diazirine-based photo-crosslinkers can be incorporated into RNA-binding proteins without significantly affecting the ability of RBPs to discriminate between two closely related RNA sequences.

Finally, we performed side-by-side comparison of conventional 254 nm UV photo-crosslinking and the diazirine-mediated photo-crosslinking using a set of commercially available UV light sources. For the conventional crosslinking, a photo-crosslinker equipped with a low pressure 254 nm mercury UV lamp with an irradiation output of ≈0.22 J cm^{-2} min^{-1} was used. The diazirine-mediated crosslinking was performed using a broad-spectrum 1 kW mercury/xenon lamp equipped with a 345 nm cutoff filter (see Table S2 for t details). When the complex of wild-type IRP1 and FTH-IRE was irradiated with 254 nm UV light at a dosage similar to those used in RIC or CLIP protocols[28] (irradiation time 1.2 min; ≈0.25 J cm^{-2}), the formation of the crosslinked product (>100 kDa) in combination with a fragmentation product (<70 kDa) was observed using denaturing SDS-PAGE (Figure 5A, lane 4). When the same wild-type IRP1–IRE complex was irradiated with longer-wavelength 345 nm UV light, no crosslinking product was observed, as expected (lane 8). A striking difference was observed for the DiAzKs mutants of IRP1, where the formation of the single crosslinking product was evident upon irradiation with 345 nm UV light for 1 min (lanes 10 and 12). Notably, the yield of the crosslinked product was visibly higher for the IRP1(A687-DiAzKs) mutant compared with the wild-type protein upon

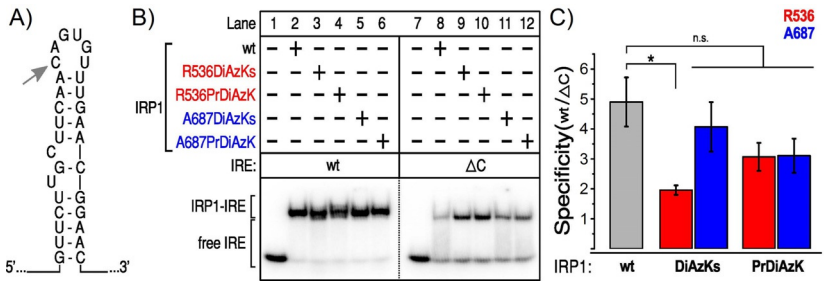

Figure 4. Binding specificity. A) The structure of the ferritin heavy chain IRE; arrow points the cytidine residue essential for the IRP1 binding. B) EMSA gel showing binding of the wild-type and the unnatural amino acid mutants of IRP1 to the wild-type and the ΔC ferritin heavy chain IRE (protein concentration was 50 nM in lanes 2–6 and 8–12); native PAGE, radioautography. C) The specificity of binding of the studied mutants measured as [fraction unbound (IRE-ΔC)]/[fraction unbound (wt-IRE)]. $^*p<0.05$, n.s.: not significant.

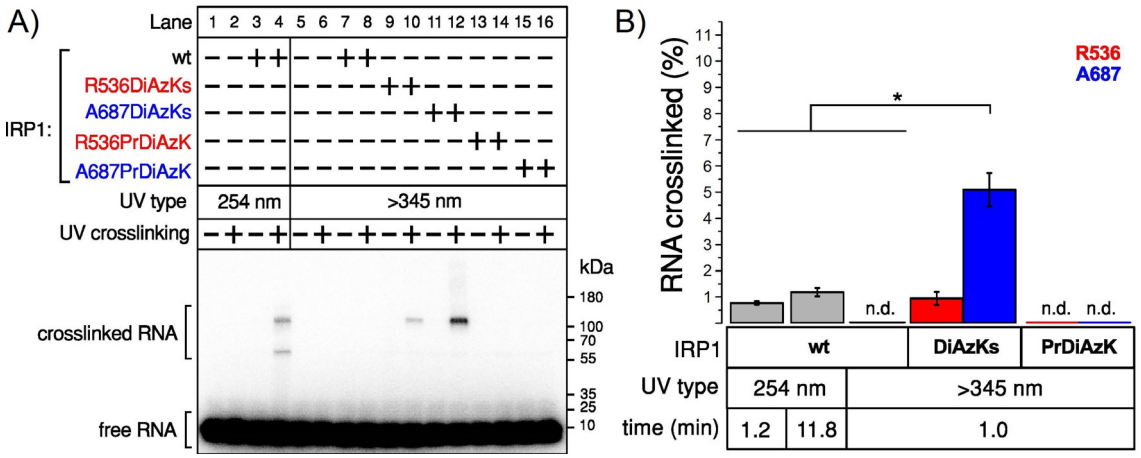

Figure 5. A) Denaturing mobility shift gels showing the UV-dependent formation of covalently crosslinked RNA–protein complexes; SDS-PAGE, radioautography. B) The effect of crosslinking time and UV type on the yield of crosslinking products. $*p < 0.05$, n.d.: not detectable.

conventional crosslinking. To our surprise, no crosslinking product was observed for the PrDiAzK mutants (lanes 14 and 16), despite the very minor difference of one methylene (-CH_2-) group in the distance from the crosslinking group to the protein backbone. Potentially, the additional propargyl group of the PrDiAzK makes the contact between the active carbene intermediate and the RNA less efficient by introducing steric clashes. The quantification of crosslinked products that can be obtained with the different crosslinking techniques (Figure 5B) shows that the conventional crosslinking yields less than 1% of the RNA crosslinked and this amount did not increase significantly upon a tenfold increase of applied energy ($\approx$2.5 J cm^{-2}, 11.8 min of irradiation). At the same time, the combination of the >345 nm UV light and A687DiAzKs mutant resulted in an approximately sevenfold higher yield of the crosslinked RNA. Additional time-course measurements showed that the irradiation time of 1 minute is sufficient to achieve the maximal amount of photo-crosslinking product (Figure S3), and prolonged irradiation gave no further benefits. We also tested the compatibility of the diazirine-mediated RNA-protein photo-crosslinking with a commercially available UV photo-crosslinker equipped with 365 nm mercury bulbs (Table S2), the instruments which are widespread in RNA laboratories due to the applications in the PAR-CLIP protocol. A time-course measurement indicated that the diazirine-mediated crosslinking can be performed using this light source (Figure S4A), although the crosslinking kinetics was much slower compared with the mercury/xenon lamp, with a reaction half-life of about 8 minutes (Figure S4B).

In this study, we show that artificial diazirine-based amino acids can be successfully applied for enhanced RNA–protein photo-crosslinking. If the labeling position is rationally selected, the insertion of the unnatural amino acid residue does not affect the binding affinity nor the specificity of the labeled RBP. A combination of the unnatural amino acid DiAzKs as a photoreactive label and appropriate light source gives an increase in the yield of the crosslinked product, which might help to overcome limitations of conventional 254 nm UV photo-crosslinking. This is particularly important in studies of lowly abundant RBPs and RNAs. Moreover, we envision that the described diazirine-mediated crosslinking could be performed in living cells and then integrated into the experimental pipeline of the CLIP methods,[5] where immunoprecipitation of a DiAzKs-labeled RBP of interest followed by RNA sequencing could be used for enhanced detection of RNA-protein contacts taking place in living cells. Finally, because the amber stop codon suppression techniques are developing rapidly and are becoming available in the growing number of model organisms and systems, the described technique could potentially be applied for RNA–protein photo-crosslinking in an organismal context.

Acknowledgements

D.D. was supported by a fellowship from the EMBL Interdisciplinary Postdoc programme (EI3POD) under Marie Skłodowska-Curie Actions COFUND (grant no. 664726). This work was supported in part by SPP1623 funded by the Deutsche Forschungsgemeinschaft (DFG). We are grateful to the staff of the EMBL Protein Expression and Purification Core Facility for their excellent technical assistance. We thank Dr. Thomas Schwarzl for help with statistical analysis. We are grateful to members of the Schultz and Hentze research groups for critical comments.

Conflict of Interest

The authors declare no conflict of interest.

Keywords: amino acids · click chemistry · photoaffinity labeling · protein modifications · RNA

[1] a) M. W. Hentze, A. Castello, T. Schwarzl, T. Preiss, *Nat. Rev. Mol. Cell Biol.* **2018**, *19*, 327–341; b) F. Gebauer, M. W. Hentze, *Nat. Rev. Mol. Cell Biol.* **2004**, *5*, 827–835; c) S. Gerstberger, M. Hafner, T. Tuschl, *Nat. Rev. Genet.* **2014**, *15*, 829–845; d) T. Glisovic, J. L. Bachorik, J. Yong, G. Dreyfuss, *FEBS Lett.* **2008**, *582*, 1977–1986.

[2] G. G. Tartaglia, *Front. Mol. Biosci.* **2016**, *3*, 24.
[3] a) D. Marchese, N. S. de Groot, N. Lorenzo Gotor, C. M. Livi, G. G. Tartaglia, *Wiley Interdiscip. Rev. RNA* **2016**, *7*, 793 – 810; b) C. Lin, W. O. Miles, *Nucleic Acids Res.* **2019**, *47*, 5490 – 5501.
[4] a) A. Castello, B. Fischer, K. Eichelbaum, R. Horos, B. M. Beckmann, C. Strein, N. E. Davey, D. T. Humphreys, T. Preiss, L. M. Steinmetz, J. Krijgsveld, M. W. Hentze, *Cell* **2012**, *149*, 1393 – 1406; b) J. I. Perez-Perri, B. Rogell, T. Schwarzl, F. Stein, Y. Zhou, M. Rettel, A. Brosig, M. W. Hentze, *Nat. Commun.* **2018**, *9*, 4408; c) T. Conrad, A.-S. Albrecht, V. R. de Melo Costa, S. Sauer, D. Meierhofer, U. A. Ørom, *Nat. Commun.* **2016**, *7*, 11212.
[5] a) F. C. Y. Lee, J. Ule, *Mol. Cell* **2018**, *69*, 354 – 369; b) R. B. Darnell, *Wiley Interdiscip. Rev. RNA* **2010**, *1*, 266 – 286.
[6] I. Saito, T. Matsuura, *Acc. Chem. Res.* **1985**, *18*, 134 – 141.
[7] E. C. Wheeler, E. L. Van Nostrand, G. W. Yeo, *Wiley Interdiscip. Rev. RNA* **2018**, *9*, e1436.
[8] I. G. Pashev, S. I. Dimitrov, D. Angelov, *Trends Biochem. Sci.* **1991**, *16*, 323 – 326.
[9] a) M. Hafner, M. Landthaler, L. Burger, M. Khorshid, J. Hausser, P. Berninger, A. Rothballer, M. Ascano, Jr., A.-C. Jungkamp, M. Munschauer, A. Ulrich, G. S. Wardle, S. Dewell, M. Zavolan, T. Tuschl, *Cell* **2010**, *141*, 129 – 141; b) M. Ascano, M. Hafner, P. Cekan, S. Gerstberger, T. Tuschl, *Wiley Interdiscip. Rev. RNA* **2012**, *3*, 159 – 177.
[10] Selected examples: a) M. C. Willis, B. J. Hicke, O. C. Uhlenbeck, T. R. Cech, T. H. Koch, *Science* **1993**, *262*, 1255 – 1257; b) M. M. Hanna, Y. Zhang, J. C. Reidling, M. J. Thomas, J. Jou, *Nucleic Acids Res.* **1993**, *21*, 2073 – 2079; c) P. V. Sergiev, I. N. Lavrik, V. A. Wlasoff, S. S. Dokudovskaya, O. A. Dontsova, A. A. Bogdanov, R. Brimacombe, *RNA* **1997**, *3*, 464 – 475; d) J. Imig, A. Brunschweiger, A. Brümmer, B. Guennewig, N. Mittal, S. Kishore, P. Tsikrika, A. P. Gerber, M. Zavolan, J. Hall, *Nat. Chem. Biol.* **2015**, *11*, 107 – 114; e) K. Nakamoto, Y. Ueno, *J. Org. Chem.* **2014**, *79*, 2463 – 2472; f) H. S. Jeong, G. Hayashi, A. Okamoto, *ACS Chem. Biol.* **2015**, *10*, 1450 – 1455; g) K. Nakamoto, K. Minami, Y. Akao, Y. Ueno, *Chem. Commun.* **2016**, *52*, 6720 – 6722; h) A. E. Arguello, A. N. DeLiberto, R. E. Kleiner, *J. Am. Chem. Soc.* **2017**, *139*, 17249 – 17252; i) F. Muttach, F. Mäsing, A. Studer, A. Rentmeister, *Chem. Eur. J.* **2017**, *23*, 5988 – 5993.
[11] J. W. Chin, *Nature* **2017**, *550*, 53 – 60.
[12] a) K. Lang, J. W. Chin, *Chem. Rev.* **2014**, *114*, 4764 – 4806; b) A. Dumas, L. Lercher, C. D. Spicer, B. G. Davis, *Chem. Sci.* **2015**, *6*, 50 – 69; c) H. Xiao, P. G. Schultz, *Cold Spring Harbor Perspect. Biol.* **2016**, *8*, a023945.
[13] N. D. Pham, R. B. Parker, J. J. Kohler, *Curr. Opin. Chem. Biol.* **2013**, *17*, 90 – 101.
[14] Selected examples: a) C. Chou, R. Uprety, L. Davis, J. W. Chin, A. Deiters, *Chem. Sci.* **2011**, *2*, 480 – 483; b) T. Yanagisawa, N. Hino, F. Iraha, T. Mukai, K. Sakamoto, S. Yokoyama, *Mol. BioSyst.* **2012**, *8*, 1131 – 1135; c) M. Zhang, S. Lin, X. Song, J. Liu, Y. Fu, X. Ge, X. Fu, Z. Chang, P. R. Chen, *Nat. Chem. Biol.* **2011**, *7*, 671 – 677; d) C. M. Joiner, M. E. Breen, J. Clayton, A. K. Mapp, *ChemBioChem* **2017**, *18*, 181 – 184; e) M. Suchanek, A. Radzikowska, C. Thiele, *Nat. Methods* **2005**, *2*, 261 – 268; f) I. Coin, V. Katritch, T. Sun, Z. Xiang, S. Y. Fai, M. Beyermann, S. C. Raymond, L. Wang, *Cell* **2013**, *155*, 1258 – 1269.
[15] L. Dubinsky, B. P. Krom, M. M. Meijler, *Bioorg. Med. Chem.* **2012**, *20*, 554 – 570.
[16] a) H.-w. Ai, W. Shen, A. Sagi, P. R. Chen, P. G. Schultz, *ChemBioChem* **2011**, *12*, 1854 – 1857; b) C. Koehler, P. F. Sauter, M. Wawryszyn, G. E. Girona, K. Gupta, J. J. M. Landry, M. H.-Y. Fritz, K. Radic, J.-E. Hoffmann, Z. A. Chen, J. Zou, P. S. Tan, B. Galik, S. Junttila, P. Stolt-Bergner, G. Pruneri, A. Gyenesei, C. Schultz, M. B. Biskup, H. Besir, V. Benes, J. Rappsilber, M. Jechlinger, J. O. Korbel, I. Berger, S. Braese, E. A. Lemke, *Nat. Methods* **2016**, *13*, 997.
[17] J.-E. Hoffmann, D. Dziuba, F. Stein, C. Schultz, *Biochemistry* **2018**, *57*, 4747 – 4752.
[18] T. Plass, S. Milles, C. Koehler, C. Schultz, E. A. Lemke, *Angew. Chem. Int. Ed.* **2011**, *50*, 3878 – 3881; *Angew. Chem.* **2011**, *123*, 3964 – 3967.
[19] a) M. W. Hentze, M. U. Muckenthaler, B. Galy, C. Camaschella, *Cell* **2010**, *142*, 24 – 38; b) M. W. Hentze, L. C. Kühn, *Proc. Natl. Acad. Sci. USA* **1996**, *93*, 8175 – 8182.
[20] W. E. Walden, A. I. Selezneva, J. Dupuy, A. Volbeda, J. C. Fontecilla-Camps, E. C. Theil, K. Volz, *Science* **2006**, *314*, 1903.
[21] Z. M. Hostetler, J. J. Ferrie, M. R. Bornstein, I. Sungwienwong, E. J. Petersson, R. M. Kohli, *ACS Chem. Biol.* **2018**, *13*, 2855 – 2861.
[22] N. K. Gray, S. Quick, B. Goossen, A. Constable, H. Hirling, L. C. Kühn, M. W. Hentze, *Eur. J. Biochem.* **1993**, *218*, 657 – 667.
[23] C. Robichon, J. Luo, T. B. Causey, J. S. Benner, J. C. Samuelson, *Appl. Environ. Microbiol.* **2011**, *77*, 4634 – 4646.
[24] C. C. Philpott, R. D. Klausner, T. A. Rouault, *Proc. Natl. Acad. Sci. USA* **1994**, *91*, 7321.
[25] M. A. Khan, W. E. Walden, E. C. Theil, D. J. Goss, *Sci. Rep.* **2017**, *7*, 8532.
[26] E. Jankowsky, M. E. Harris, *Nat. Rev. Mol. Cell Biol.* **2015**, *16*, 533 – 544.
[27] M. W. Hentze, S. W. Caughman, T. A. Rouault, J. G. Barriocanal, A. Dancis, J. B. Harford, R. D. Klausner, *Science* **1987**, *238*, 1570.
[28] A. Castello, R. Horos, C. Strein, B. Fischer, K. Eichelbaum, L. M. Steinmetz, J. Krijgsveld, M. W. Hentze, *Nat. Protoc.* **2013**, *8*, 491 – 500.

Manuscript received: September 10, 2019
Accepted manuscript online: October 28, 2019
Version of record online: November 26, 2019

